JURNAL INFOTEL
VOL. 18, NO. 2, MAY 213, PP. 213–225. DOI:10.20895/INFOTEL.V18I2.1319

RESEARCH ARTICLE

A Comparative Analysis of YOLOv5 and YOLOv8 for Watermelon Sweetness Prediction Based on Their Field Spot

Rahmad Dawood[1,2,*], Maya Fitria[1,2], Muhammad Hafez Al-Assad[1], Yudi Candra[1], Silvia Roza[1]

[1]Department Electrical and Computer Engineering, Universitas Syiah Kuala, 23111, Indonesia

[2]Interactive Intelligent Systems Research Group, Universitas Syiah Kuala, 23111, Indonesia

*Corresponding email: rahmad.dawood@usk.ac.id

Received: January 26, 2026; Revised: March 27, 2026; Accepted: May 18, 2026.

Abstract: Despite high market demand, accurately determining the sweetness and ripeness of watermelons remains a challenge. Traditionally, these qualities are identified through manual inspection of weight, acoustic tapping, or visual characteristics such as rind color and field spots. The field spot is the area where the fruit rests on the ground during growth; its transition from white to yellow serves as a key indicator of the natural ripening process and the accumulation of internal sugars. However, these methods are subjective, time-consuming, and prone to human error. This research utilizes object detection algorithms to classify watermelon sweetness levels based on field spot characteristics, with the aim of a more objective and consistent evaluation. The study evaluates the YOLOv5 and YOLOv8 architectures using a dataset of 333 images categorized into sweet and non-sweet classes. Model performance was assessed using precision, recall, and mean Average Precision (mAP@50 and mAP @ 50-90). The findings indicate that YOLOv5 outperformed YOLOv8, achieving mAP@50 values of 85.3% and 81.9%, respectively. Furthermore, YOLOv5 demonstrated higher training efficiency. These results suggest that YOLOv5 offers a more robust and deployable solution for non-destructive agricultural quality assessment.

Keywords: Fruit Quality Classification, Non-destructive Testing, Image Classification, Watermelon Sweetness Classification, Field Spot Characteristics, YOLOv5, YOLOv8.

 ISSN: 2085-3688; e-ISSN: 2460-0997

1 Introduction

According to the United Nations' Food and Agriculture Organization (FAO), in 2018, watermelons were grown on 3.2 million acres worldwide, producing more than 100 million tons [1,2]. Asia represented more than 80% of this production [3,4]. The fruit is a source of essential nutrients, such as vitamins B, C, and E, along with minerals such as calcium, iron, and zinc [5]. These health benefits, coupled with its taste profile and visual attributes—with flesh colors ranging from red to pink and yellow—contribute to its widespread consumption. In Indonesia, watermelon consumption increased by 6.14% between 2014 and 2018 [6], reflecting the continued demand of consumers. To remain competitive, watermelon quality must consistently meet national and international standards, with sweetness being a critical factor for consumer acceptance.

To assess current practices for evaluating watermelon quality, interviews were conducted in several fruit markets in Banda Aceh, agrotourism areas in Aceh Besar, and the UPTD Balai Benih Hortikultura Tanaman Pangan dan Tanaman Perkebunan. These interviews indicated that ripeness and sweetness are typically judged through visual cues, such as the color of the rind and the appearance of the field spot, as well as physical attributes, including weight and the sound produced by tapping. Because these traditional methods are based on individual perception, they are highly subjective and lack standardized categorization. In contrast, the Indonesian National Standard (SNI) quantifies the sweetness using Total Soluble Solids (TSS), requiring a minimum of 8% Brix [7]. However, determining Brix values requires cutting the fruit to extract juice samples, which is a destructive process. Consequently, a more objective and non-destructive approach is required to evaluate watermelon quality.

Various non-destructive approaches have been explored to assess fruit sweetness, ranging from spectral and acoustic analysis to advanced machine learning. For watermelon ripeness detection, Jie et al. utilized VIS/NIR spectral imaging to achieve 88.1% accuracy [8], while Albert-Weiß combined acoustic resonance with deep learning to classify ripeness with 96% accuracy [9]. Traditional machine learning has also been applied; for instance, Nazulan et al. used K-Means clustering on external visual features—specifically color, shape, and field spot—to detect sweetness, although their reported 84.62% accuracy was constrained by a small dataset of 15 images [10]. More recently, deep Convolutional Neural Networks (CNNs) have shown significant promise in this domain. Muchallil et al. demonstrated the efficacy of EfficientNet-B4 and ResNet-50 for pineapple sweetness classification, achieving 84.09% accuracy [11]. Building on these architectures for watermelons, Fitria et al. compared EfficientNet-B4, ResNet-50, and ShuffleNet-V2, with ShuffleNet-V2 achieving 88.06% accuracy [12]. A subsequent study by the same authors introduced the EfficientNet-B7 architecture, which substantially improved the classification accuracy of watermelon sweetness to 98.88% [13].

Despite the high classification accuracy reported in previous studies, many of these approaches rely on image-level classification models evaluated in controlled settings, limiting their applicability in real-world environments. In practice, the automatic localization of key visual indicators of ripeness—particularly the field spot—is essential to support real-time, non-destructive quality assessment systems. To address this limitation, this study proposes a watermelon sweetness classification model utilizing the You Only Look Once (YOLO) object detection algorithm, using the proven efficacy of deep learning in complex computer vision tasks [14]. YOLO is specifically suited for this application due to its ability

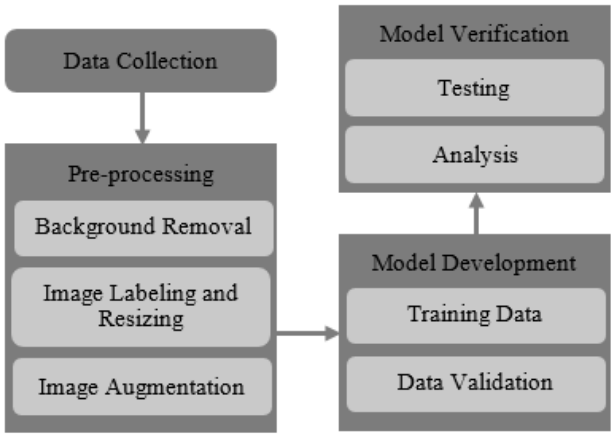

Figure 1: Research flowchart.

to rapidly identify and delineate target objects using bounding boxes [15]. YOLOv5 and YOLOv8 were selected for this research, as both architectures have demonstrated superior accuracy compared to previous iterations [16–18]. YOLOv5 provides an established balance of high detection accuracy and robust real-time processing speed [19]. Furthermore, YOLOv8 offers a significant architectural advancement with its anchor-free detection head, which simplifies the detection pipeline and further enhances precision. The results of this study are expected to serve as a basis for future research, contributing to the practical development of automated agricultural quality-sorting machinery and applications.

2 Research Method

The research methodology consists of four primary stages: data collection, data preprocessing, model development, and model verification (Figure 1).

2.1 Watermelon Characteristics and Data Collection Scenario

Based on interviews and field observations, two traditional methods are commonly used to determine watermelon maturity and sweetness. The first involves evaluating the acoustic response produced by tapping the lower section of the fruit; a mature watermelon typically generates a deeper, more resonant sound. The second method relies on the visual inspection of the field spot. A large, yellowish field spot signifies full maturation on the vine, whereas immature watermelons are characterized by smaller, white field spots. Figure 2 illustrates the visual comparison between high-sweetness and low-sweetness samples.

While these two traditional methods are widely used, the standard quantitative metric for sweetness is the Brix value, measured using a refractometer. Consequently, Brix measurements were utilized in this study to establish a ground truth for each sample. Immediately following image acquisition, a section of the watermelon was removed to extract juice

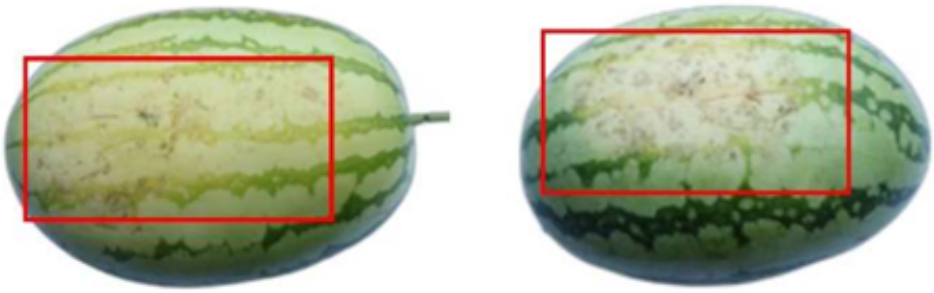

Figure 2: Field spot characteristics: high-sweetness (left) and low-sweetness (right).

from the fruit flesh. This juice was then analyzed using a digital refractometer to obtain the Brix value for each sample. This procedure is illustrated in Figure 3.

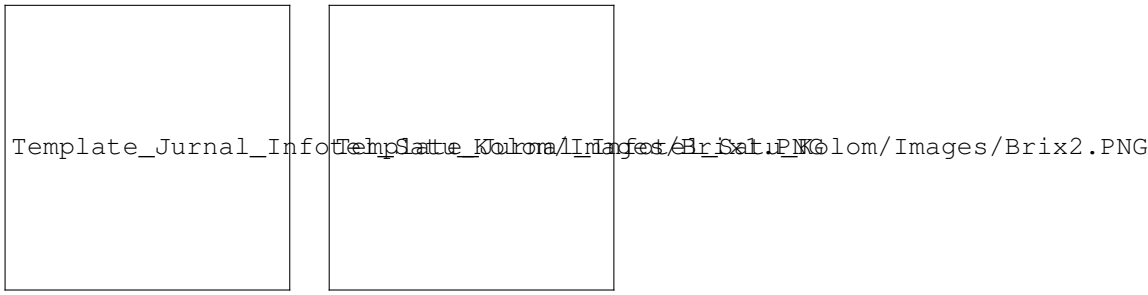

Figure 3: Brix measurement procedure: (a) juice extraction and (b) refractometer reading.

This study classifies watermelon sweetness levels based on the visual characteristics of the field spot, with samples divided into two distinct categories: high-sweetness and low-sweetness. The Brix values obtained through the procedure described above provide the objective basis for these categories. According to the criteria established by the Indonesian National Standard (SNI 7420:2009), a Brix value exceeding 8% is categorized as high-sweetness, while a value of 8% or lower is classified as low-sweetness [7].

The dataset utilized in this study is a primary collection consisting of watermelon specimens photographed shortly after harvest. All image acquisition was conducted under natural light at a distance of 40 cm between the specimen and the camera. A Canon EOS M10 camera was employed, configured with an aperture of $f/3.5$ and a focal length of 16 mm. Each specimen was photographed from six perspectives: front, back, left, right, top, and bottom. The resulting images maintain a resolution of 5184 × 3456 pixels. This acquisition setup is illustrated in Figure 4. Immediately following image acquisition, the Brix value of each specimen was measured using a refractometer to establish ground-truth sweetness levels. The final dataset comprises a total of 151 images, partitioned into 87 high-sweetness samples (labeled as "sweet") and 64 low-sweetness samples (labeled as "not-sweet").

Figure 4: Data acquisition setup for the watermelon dataset.

2.2 Data Preprocessing

A four-step preprocessing pipeline was applied to the collected raw images to generate a clean dataset. First, background removal was performed using the Rembg Python library [20]. Subsequently, the Roboflow platform [21] was employed for image annotation, resizing, and augmentation. Each image was labeled and assigned to either the high-sweetness or low-sweetness class. All images were then resized to a resolution of 640 × 640 pixels using a center-crop fill method, ensuring the primary object of interest was retained and centered.

To introduce data diversity and mitigate class imbalance, the standardized images were augmented. This augmentation was performed randomly using the Roboflow platform, employing several techniques as illustrated in Figure 5): (a) horizontal flipping, (b) vertical flipping, (c) free rotation between -15°and 15°, (d) 90°rotations (clockwise and counter-clockwise) alongside a 180°inversion, (e) a 1-pixel blur, (f) 0.5% noise addition, and (g) shearing. The final size of the augmented dataset is detailed in Table 1. Finally, the dataset was partitioned into training, validation, and testing subsets using a 64:18:18 split, as presented in Table 2.

Table 1: Total number of original and augmented images per class.

Dataset	Sweet Class	Not Sweet Class	Total
Original	87	64	151
Augmented	167	166	333

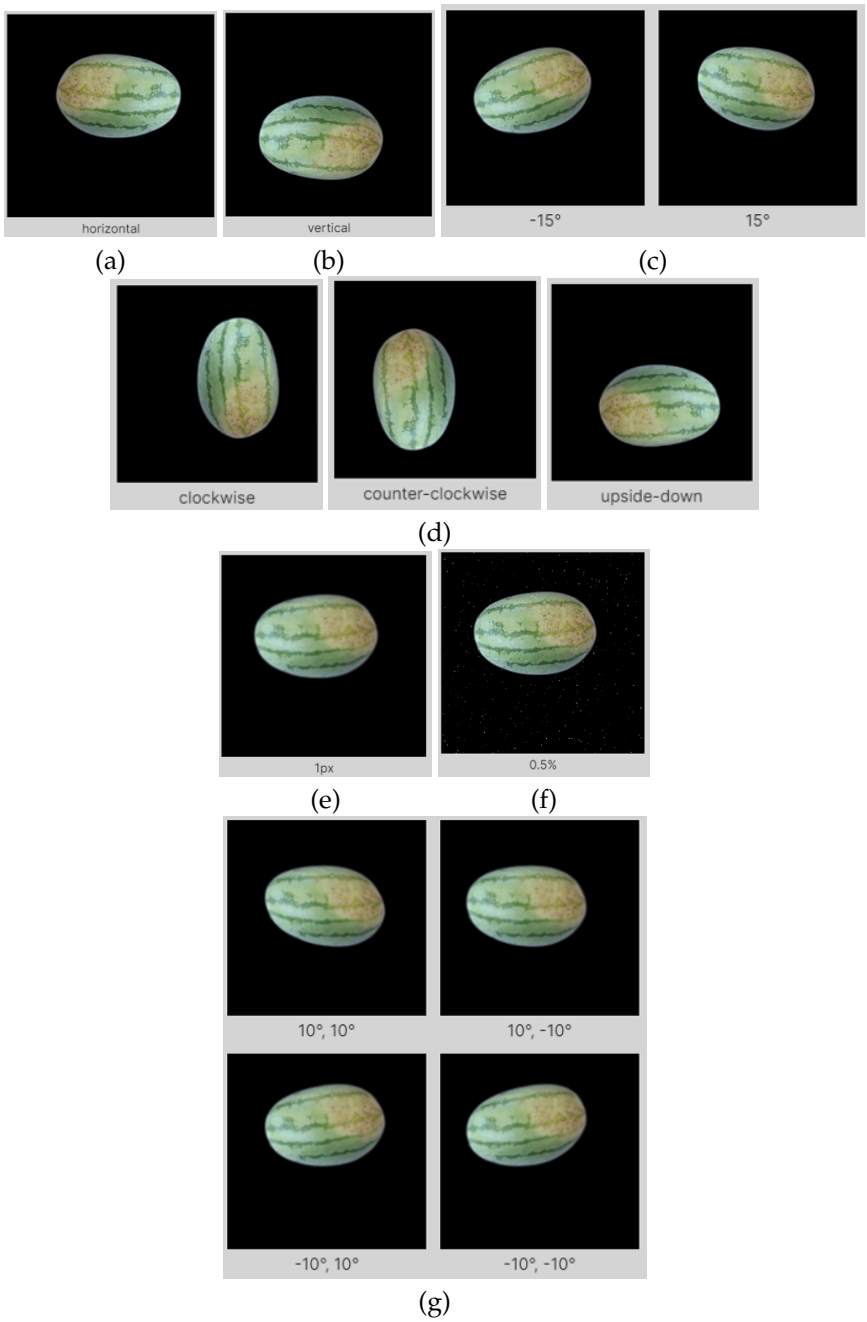

Figure 5: Sample images generated using the data augmentation techniques in this study.

Table 2: Dataset distribution across training, validation, and testing subsets.

Dataset	Sweet Class	Not Sweet Class	Total
Training	107	106	213
Validation	30	30	60
Testing	30	30	60
Total	167	166	333

2.3 Model Development

During the model development stage, 213 images were used for training and 60 images for validation. Rather than training from scratch, a transfer learning approach was adopted using pre-trained YOLOv5 and YOLOv8 models. Hyperparameter tuning was performed to optimize the models, with the selected configurations detailed in Table 3. This tuning and model development process was executed on a server with an NVIDIA RTX A6000 GPU; the hardware and software specifications are detailed in Table 4. Throughout training, the validation subset was used concurrently to monitor model performance and mitigate the risk of overfitting [22].

Table 3: Hyperparameter configurations.

Parameter	YOLOv5	YOLOv8
Optimizer	AdamW	AdamW
Image Size	416	416
Epoch	100	100
Batch Size	16	16
Learning Rate	10^{-2}, 10^{-3}, 10^{-4}	10^{-2}, 10^{-3}, 10^{-4},
Momentum	0.937	0.937
Architecture Version	YOLOv5	YOLOv8

2.4 Model Verification

The objective of the model evaluation phase was to assess the performance of the developed models using a dedicated test dataset. This dataset comprised 60 watermelon images, encompassing both the sweet and non-sweet classes. Performance was evaluated based on precision, recall, Mean Average Precision (mAP@50 and mAP@50-95), and inference time.

The mAP@50 score was calculated at a fixed Intersection over Union (IoU) threshold of 0.5, where a detection is considered a true positive if the overlap between the predicted and ground-truth bounding boxes is at least 50%. Conversely, mAP@50-95 was calculated by averaging the AP across a range of IoU thresholds from 0.5 to 0.95 in 0.05 increments, providing a more robust measure of localization accuracy. Finally, confusion matrices were generated to analyze the classification performance for the sweet and not-sweet categories, illustrating the distribution of true positives, false positives, and false negatives.

Table 4: Hardware and software specifications.

Hardware Specification
1 unit PC/Laptop equipped with AMD Ryzen 7 5800H (8C / 16T, 3.2 / 4.4GHz, 4MB L2 / 16MB L3), 16.00 GB RAM
Graphics NVIDIA GeForce RTX 3050 Ti 4GB GDDR6, Boost Clock 1485 / 1695MHz, TGP 95W
Server SSH Keio University sfc-gpu.ai3.net GPU NVIDIA RTX A6000
Software Specifications
Windows 11 Home Single Language 64-bit Operating System
Python programming language (installable from python.org)
IDE Visual Studio Code
PyTorch Deep Learning Frameworks
CUDA GPU Acceleration Libraries
Additional Libraries and Tools: scikit-learn, numpy, pandas, matplotlib, tqdm, etc.

3 Results

Table 5 presents the evaluation metrics from the model development, including precision, recall, mAP@50, mAP@50-95, and inference time (speed) for each architecture. As established in the object detection literature, higher mAP values indicate better model performance [23]. The results demonstrate that YOLOv5 consistently outperformed YOLOv8 in mAP@50 and mAP@50-95 across all tested learning rates. Notably, YOLOv5 achieved its peak performance at a learning rate of 10^{-2}, with an mAP@50 of 0.890 and an mAP@50-95 of 0.853. Additionally, the data reveals a direct relationship between the learning rate and overall accuracy: reducing the learning rate resulted in a corresponding decrease in mAP scores. While YOLOv5 exhibited higher precision across all learning rates, YOLOv8 demonstrated higher recall at learning rates of 10^{-2} and 10^{-4}.

Table 5: Performance of YOLOv5 and YOLOv8 at various learning rates.

Architecture	**Learning Rates**	**Precision**	**Recall**	**mAP@50**	**mAP@50-95**	**Speed (s)**
YOLOv5	10^{-2}	0.868	0.833	0.890	0.853	944
	10^{-3}	0.869	0.789	0.871	0.836	1206
	10^{-4}	0.717	0.847	0.857	0.812	1298
YOLOv8	10^{-2}	0.702	0.917	0.856	0.819	1415
	10^{-3}	0.748	0.764	0.856	0.815	1341
	10^{-4}	0.616	0.913	0.832	0.803	1370

As shown in Table 5, the training time for YOLOv5 was consistently shorter than that of YOLOv8 across all learning rates. YOLOv5 achieved its shortest training time at a learning rate of 10^{-2}, completing the process in 944 seconds. In contrast, the longest training time was recorded by YOLOv8 at this same learning rate, requiring 1,415 seconds.

Figures 6 and 7 compare the training processes of both YOLO architectures over 100 epochs at a learning rate of 10^{-2}. Given that the loss curves demonstrate clear convergence and the mAP metrics reach a stable plateau during the final iterations, training

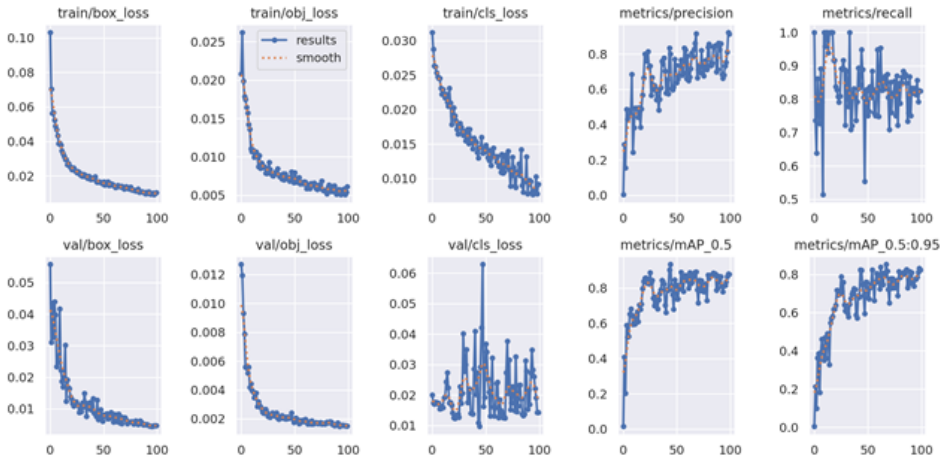

Figure 6: YOLOv5 training curves at a learning rate of 10^{-2}.

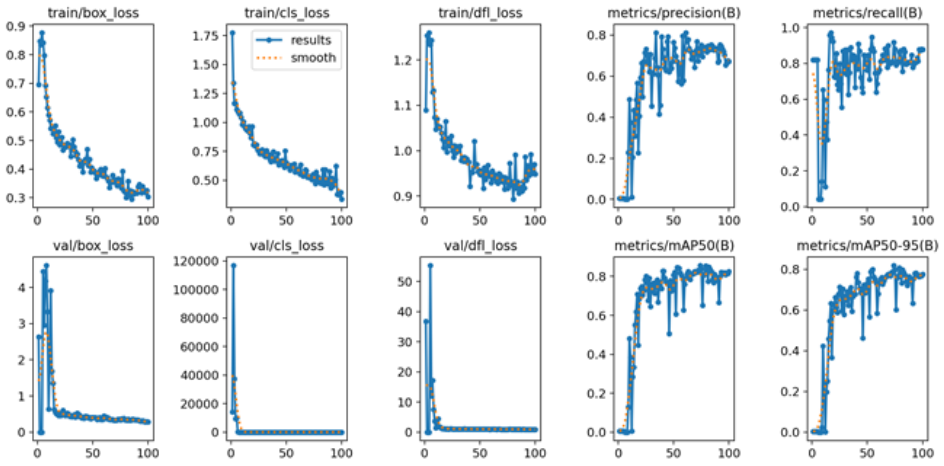

Figure 7: YOLOv8 training curves at a learning rate of 10^{-2}.

was concluded to prevent potential overfitting and optimize computational efficiency. A comparison of these figures demonstrates that YOLOv5 achieved better final metrics than YOLOv8. During YOLOv5 training, the overall loss values decreased gradually, although fluctuations were observed in the training class loss and Distribution Focal Loss (DFL). Furthermore, the validation box, validation class, and validation DFL losses exhibited rapid declines starting at epochs 20, 10, and 10, respectively. Despite the steady convergence of the training and validation losses, YOLOv5 displayed fluctuating curves for precision, recall, and mAP scores. These fluctuations typically indicate underlying factors such as training instability, variations in data quality, hyperparameter sensitivity, or batch-to-batch variability.

4 Discussion

The primary objective of this study was to develop an automated, non-destructive method for evaluating watermelon quality based on visual features, specifically the field spot. A transfer learning approach was adopted, utilizing the YOLOv5 and YOLOv8 architectures. Training was performed on a primary dataset collected specifically for this research.

The study results indicate that YOLOv5 consistently outperformed YOLOv8 in terms of mAP@50, mAP@50–95, and overall training efficiency. While YOLOv8 demonstrated higher recall at specific learning rates, YOLOv5 achieved an optimal balance between precision and recall, producing more stable and reliable performance. This distinct performance trade-off, where YOLOv5 prioritized precision and YOLOv8 preferred recall, can be attributed to their respective architectural designs. YOLOv5 utilizes a coupled head and an anchor-based approach, which imposes stricter criteria for object matching and leads to more reliable identifications. In contrast, YOLOv8 employs a decoupled head and an anchor-free mechanism. This design enhances sensitivity to ambiguous visual features, such as marginally visible field spots. Consequently, while YOLOv8 is more effective in ensuring that fewer potential field spots are missed, YOLOv5 maintains a more conservative confidence threshold better suited for high-precision quality grading.

The influence of the learning rate was also highly evident in the results. A learning rate of 10^{-2} yielded the best overall performance for both architectures, while smaller learning rates resulted in reduced mAP values. This finding underscores the importance of hyperparameter selection in optimizing detection performance, particularly when using datasets characterized by limited samples and natural variability in visual features.

In terms of training dynamics, the observed fluctuations in the evaluation metric curves reflect a sensitivity to the inherent variability of the dataset, specifically field spot characteristics such as differences in color intensity, shape, and illumination conditions. However, the models reached asymptotic stability by epoch 100. The absence of significant divergence between the training and validation loss curves indicates that there was no significant overfitting. Furthermore, the evaluation across various learning rates supports the overall stability of the models.

The confusion matrix analysis (see Figure 8) indicates that YOLOv5 achieved high precision in the identification of sweet watermelons (94%), while misclassification occurred more frequently within the category " not-sweet (33%). This pattern is likely attributable to subtle visual similarities between marginally sweet and non-sweet field spot appearances, suggesting that certain cases present overlapping visual features. These findings underscore both the practical capabilities and the current limitations of the model. Consequently, future research could explore the incorporation of additional visual cues or multimodal features to further enhance classification accuracy and ensure consistent performance across both categories.

From a practical perspective, utilizing object detection to specifically target the watermelon field spot, rather than relying on image-level classification, offers a significant advantage. This approach is in alignment with traditional agricultural practices, where field spot observation is a standard indicator to estimate maturity. Furthermore, the lightweight nature of the YOLO architectures utilized in this study enables potential integration into real-time systems, such as mobile or API-based applications for automated quality assessment. Consequently, beyond a comparative accuracy analysis, this study demonstrates the feasibility of developing deployable, non-invasive agricultural AI systems.

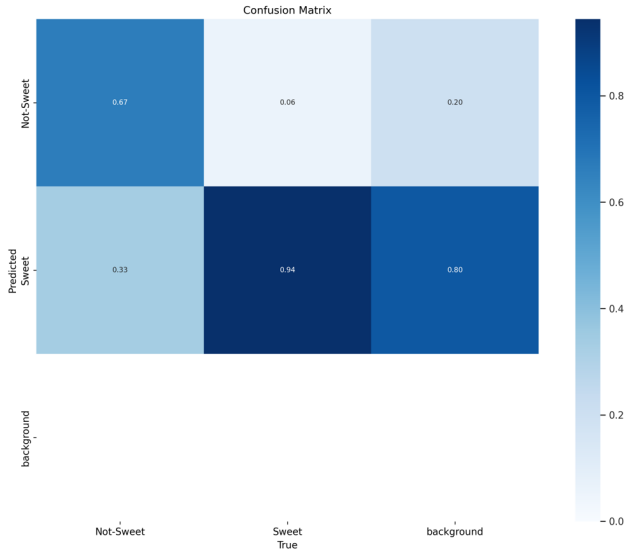

Figure 8: Confusion matrix for YOLOv5.

5 Conclusion

This study evaluated two YOLO architectures, specifically YOLOv5 and YOLOv8, to classify watermelon quality based on sweetness levels. The results demonstrate that YOLOv5 achieved the most effective balance in the precision, recall, mAP@50, and mAP@50:95 metrics, while maintaining a higher training efficiency, particularly at a learning rate of 10^{-2}. Although YOLOv8 exhibited high recall, its overall performance did not exceed that of YOLOv5. Analysis of the training curves revealed frequent fluctuations in the metrics of both models.

These findings offer a framework for automated watermelon quality assessment. By utilizing field spot localization for non-destructive sweetness prediction, the assessment system can facilitate intelligent sorting and standardized grading. Given the lightweight nature of the architectures employed in this study, they are highly suitable for integration into edge-computing devices or mobile platforms, enabling real-time deployment throughout the post-harvest supply chain. Future research should focus on further hyperparameter optimization and the expansion of the dataset to include diverse watermelon varieties to enhance model stability and generalization.

Acknowledgments

This research was supported by APNIC Foundation and Keio University under CBR grant scheme 2022.

References

[1] F. Bantis, A. Koukounaras, A. S. Siomos, K. Radoglou, and C. Dangitsis, "Optimal led wavelength composition for the production of high-quality watermelon and interspecific squash seedlings used for grafting," *Agronomy*, vol. 9, no. 12, p. 870, 2019.

[2] N. Helilusiatiningsih, P. S. Utomo, *et al.*, "Post harvest and technology of watermelon (citrullus lanatus) plants in integrated field laboratory faculty of agriculture kediri," *Formosa Journal of Applied Sciences*, vol. 1, no. 6, pp. 1041–1050, 2022.

[3] A. Manivannan, E.-S. Lee, K. Han, H.-E. Lee, and D.-S. Kim, "Versatile nutraceutical potentials of watermelon—a modest fruit loaded with pharmaceutically valuable phytochemicals," *Molecules*, vol. 25, no. 22, p. 5258, 2020.

[4] J. Dube, G. Ddamulira, and M. Maphosa, "Watermelon production in africa: challenges and opportunities," *International Journal of Vegetable Science*, vol. 27, no. 3, pp. 211–219, 2021.

[5] S. V. Theurkar, D. P. Gawari, and D. N. Birhade, "Watermelon as a potential nutritional horticultural crop: A comprehensive review," *World Journal of Advanced Research and Reviews*, vol. 18, no. 2, pp. 627–629, 2023.

[6] D. Ishartani, A. M. Sari, R. Arifani, *et al.*, "Partial characterization of watermelon albedo pectin extracted using citric acid combined with microwave assisted extraction," in *IOP Conference Series: Earth and Environmental Science*, vol. 518, p. 012060, IOP Publishing, 2020.

[7] B. S. N. Indonesia, "Sni 7420:2009." https://pesta.bsn.go.id/produk/detail/7630-sni74202009. Last accessed: 1 June 2024.

[8] D. Jie, W. Zhou, and X. Wei, "Nondestructive detection of maturity of watermelon by spectral characteristic using nir diffuse transmittance technique," *Scientia Horticulturae*, vol. 257, p. 108718, 2019.

[9] D. Albert-Weiß, E. Hajdini, M. Heinrich, and A. Osman, "Cnn for ripeness classfication of watermelon fruits based on acoustic testing," in *Proceedings of the Virtual 3rd International Symposium on Structural Health Monitoring and Nondestructive Testing (SHM-NDT 2020), Quebeq, QU, Canada*, pp. 25–26, 2020.

[10] W. N. S. W. Nazulan, A. L. Asnawi, H. A. M. Ramli, A. Jusoh, S. N. Ibrahim, and N. Azmin, "Detection of sweetness level for fruits (watermelon) with machine learning," in *2020 IEEE Conference on Big Data and Analytics (ICBDA)*, pp. 79–83, IEEE, 2020.

[11] S. Muchallil, S. Roza, M. H. Al-Assad, Y. Candra, M. Fitria, and R. Dawood, "Deep learning implementation for pineapple sweetness classification," in *International Conference on Data Science and Artificial Intelligence*, pp. 185–197, Springer, 2023.

[12] M. Fitria, Y. Candra, M. H. Al-Assad, S. Roza, and R. Dawood, "A deep learning-based model for classifying sweetness level of sky rocket melon: A preliminary result," in *2023 2nd International Conference on Computer System, Information Technology, and Electrical Engineering (COSITE)*, pp. 204–209, IEEE, 2023.

[13] M. Fitria, M. H. Al-Assad, Y. Candra, S. Roza, and R. Dawood, "Preliminary results of a deep learning model for classifying watermelon sweetness through field-spot detection," in *1st International Conference on Business and Technological Advancement in Industrial Revolution 4.0*, p. 43, 2023.

[14] N. Ganatra and A. Patel, "Deep learning methods and applications for precision agriculture," *Machine Learning for Predictive Analysis: Proceedings of ICTIS 2020*, pp. 515–527, 2021.

[15] T. Diwan, G. Anirudh, and J. V. Tembhurne, "Object detection using yolo: Challenges, architectural successors, datasets and applications," *multimedia Tools and Applications*, vol. 82, no. 6, pp. 9243–9275, 2023.

[16] K. Kim, K. Kim, and S. Jeong, "Application of yolo v5 and v8 for recognition of safety risk factors at construction sites," *Sustainability*, vol. 15, no. 20, p. 15179, 2023.

[17] V. D. Matta, K. V. R. R. Mudunuri, B. C. S. Sai Baba, K. B. Kiran, C. L. Veenadhari, and B. Prasanthi, "Single use plastic bottle recognition and classification using yolo v5 and v8 architectures," in *International Conference on Cognitive Computing and Cyber Physical Systems*, pp. 99–106, Springer, 2023.

[18] E. Casas, L. Ramos, E. Bendek, and F. Rivas-Echeverría, "Assessing the effectiveness of yolo architectures for smoke and wildfire detection," *IEEE Access*, 2023.

[19] J. Terven, D.-M. Córdova-Esparza, and J.-A. Romero-González, "A comprehensive review of yolo architectures in computer vision: From yolov1 to yolov8 and yolo-nas," *Machine Learning and Knowledge Extraction*, vol. 5, no. 4, pp. 1680–1716, 2023.

[20] D. Gatis, "rembg." original-date: 2020-08-10T14:38:24Z.

[21] Q. Lin, G. Ye, J. Wang, and H. Liu, "Roboflow: a data-centric workflow management system for developing ai-enhanced robots," in *Conference on Robot Learning*, pp. 1789–1794, PMLR, 2022.

[22] A. Febriana, K. Muchtar, R. Dawood, and C.-Y. Lin, "Usk-coffee dataset: a multi-class green arabica coffee bean dataset for deep learning," in *2022 IEEE International Conference on Cybernetics and Computational Intelligence (CyberneticsCom)*, pp. 469–473, IEEE, 2022.

[23] N. Chitraningrum, L. Banowati, D. Herdiana, B. Mulyati, I. Sakti, A. Fudholi, H. Saputra, S. Farishi, K. Muchtar, and A. Andria, "Comparison study of corn leaf disease detection based on deep learning yolo-v5 and yolo-v8," *Journal of Engineering and Technological Sciences*, vol. 56, no. 1, pp. 61–70, 2024.